

AD-A034 092

AIL DEER PARK N Y  
WAVEGUIDE HF LASER.(U)  
NOV 76 A STEIN  
AIL-C416-1

F/G 20/5

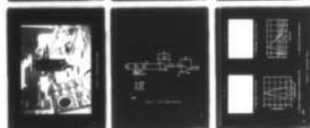
UNCLASSIFIED

N00014-76-C-0397

NL

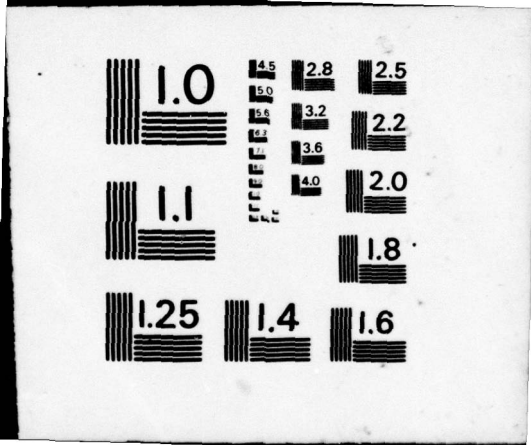
1 of 1  
4DA034092

1 of 1



END

DATE  
FILMED  
2 - 77



ADA034092

12

FC

# WAVEGUIDE HF LASER

Semiannual Report  
for period December 8, 1975 to June 7, 1976

by  
A. Stein

AIL REPORT NO. C416-1  
NOVEMBER 1976

Prepared under Contract N00014-76-C-0397  
Office of Naval Research  
Washington, D.C.

DDC  
RECEIVED  
DEC 15 1976  
A

Sponsored by  
ADVANCED RESEARCH PROJECTS AGENCY  
ARPA Order No. 1806, Amendment No. 25

DISTRIBUTION STATEMENT A  
Approved for public release  
Distribution Unlimited

AIL a division of CUTLER-HAMMER



DEER PARK, LONG ISLAND, NEW YORK 11729

1473

CONTRACT NO.: N00014-76-C-0397  
ARPA ORDER NO.: 1806, Amend. 25  
PROGRAM CODE: 6E20  
NAME OF CONTRACTOR: AIL, a division of Cutler-Hammer  
EFFECTIVE DATE OF CONTRACT: Dec. 8, 1975  
CONTRACT EXPIRATION DATE: Dec. 7, 1976  
CONTRACT AMOUNT: \$99,392  
PRINCIPAL INVESTIGATOR: Dr. A. Stein (516)-595-4405  
SCIENTIFIC OFFICER: Office of Naval Research  
800 N. Quincy Street  
Arlington, Virginia 22217  
Attn: Code 421, Dr. M.B. White

DISCLAIMER: The views and conclusions contained in this document are those of the author's and should not be interpreted as necessarily representing the official policies, either expressed or implied, of the Advanced Research Projects Agency or the U.S. Government.

ADDITION BY	
DATE	
BY	
<i>Letter on file</i>	
FOR DISTRIBUTION/AVAILABILITY USE	
D. C. OFFICE OF SPECIAL	
A	

## ABSTRACT

A purely electrical activation mechanism for HF lasers was investigated, whereby HF molecules are vibrationally excited through inelastic electron collisions in a discharge plasma. The plasma is generated by a transverse discharge inside a 1 x 1 mm rectangular channel of 8 cm length filled with a mixture of HF and an inert diluent gas. To obtain the desired plasma condition auxiliary high energy electrons are injected into the plasma.

Initial fluorescence measurements for pulsed excitation indicate that further increases in the excitation rate are necessary. The remainder of this program will be concerned with two measures to enhance the excitation rate; (1) stretching of the discharge pulse to attain better quantum energy storage, and (2) seeding of the plasma with hydrogen gas which transfers its excitation to the HF molecules.

REPORT DOCUMENTATION PAGE		READ INSTRUCTIONS BEFORE COMPLETING FORM	
1. REPORT NUMBER <b>14</b> AIL-C-416-1 ✓	2. GOVT ACCESSION NO.	3. RECIPIENT'S CATALOG NUMBER <b>9</b>	
4. TITLE (and Subtitle) <b>6</b> Waveguide HF Laser, ✓		5. TYPE OF REPORT & PERIOD COVERED Semiannual <i>rept.</i> 8 Dec 1975 - 7 June 1976 <b>3</b>	
7. AUTHOR(s) <b>10</b> A. Stein		8. CONTRACT OR GRANT NUMBER(s) <b>15</b> N00014-76-C-0397 <i>NEW</i>	
9. PERFORMING ORGANIZATION NAME AND ADDRESS ✓ AIL, division of Cutler-Hammer Deer Park, New York 11729		10. PROGRAM ELEMENT, PROJECT, TASK AREA & WORK UNIT NUMBERS <b>12</b> 43P.	
11. CONTROLLING OFFICE NAME AND ADDRESS Office of Naval Research 800 N. Quincy Street Arlington, Virginia 22217		12. REPORT DATE <b>11</b> Nov 1976	
14. MONITORING AGENCY NAME & ADDRESS (if different from Controlling Office)		13. NUMBER OF PAGES	
		15. SECURITY CLASS. (of this report) Unclassified	
		15a. DECLASSIFICATION/DOWNGRADING SCHEDULE	
16. DISTRIBUTION STATEMENT (of this Report)			
17. DISTRIBUTION STATEMENT (of the abstract entered in Block 20, if different from Report)			
18. SUPPLEMENTARY NOTES			
19. KEY WORDS (Continue on reverse side if necessary and identify by block number)  HF Laser                      Waveguide Laser			
20. ABSTRACT (Continue on reverse side if necessary and identify by block number)  A purely electrical activation mechanism for HF lasers was investigated, whereby HF molecules are vibrationally excited through inelastic electron collisions in a discharge plasma. The plasma is generated by a transverse discharge inside a 1 x 1 mm rectangular channel of 8 cm length filled with a mixture of HF and an inert diluent gas. To obtain the desired plasma condition auxiliary high energy electrons are injected			

over

int

20. ABSTRACT (continued)

into the plasma.

Initial fluorescence measurements for pulsed excitation indicate that further increases in the excitation rate are necessary. The remainder of this program will be concerned with two measures to enhance the excitation rate; (1) stretching of the discharge pulse to attain better quantum energy storage, and (2) seeding of the plasma with hydrogen gas which transfers its excitation to the HF molecules.

## TABLE OF CONTENTS

	<u>Page</u>
I. INTRODUCTION	1
II. BACKGROUND AND ANALYSIS	5
III. LASER DEVICE AND EXPERIMENTAL EFFORT	16
Summary	26
References	28



## LIST OF ILLUSTRATIONS

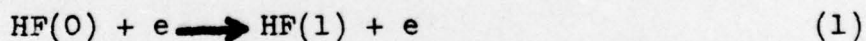
<u>Figure</u>		<u>Page</u>
1	Laser Head - Schematic	29
2	Laser Head - View No. 1	30
3	Laser Head - View No. 2	31
4	Discharge Data	32
5	Experimental Set-Up	33
6	Fluorescence Radiometer	34
7	Photo Signal Amplifier	35
8	Fluorescence Data	36

## I. INTRODUCTION

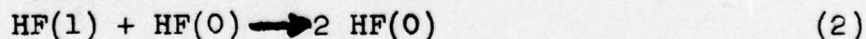
The object of this program is to develop a novel HF waveguide laser which employs electron collisional activation of HF molecules in a discharge rather than the usual chemical reaction between hydrogen and fluorine. A transverse discharge is formed in a small capillary vessel filled with HF gas heavily diluted in helium. Such a device can be as compact as small CO<sub>2</sub> systems, an obvious improvement over the present chemical HF lasers. In addition, a waveguide HF oscillator offers the intrinsic stability of discharge lasers when operated sealed off.

A self contained, stable HF laser oscillating at 2.6-2.9 μm is desirable for application in pointing and tracking, optical radar, communication, and general surveillance. Furthermore, the discharge technology developed on this program may be applied to other important laser species. In particular, DF may replace the HF molecules to achieve laser outputs at 3.6-4.0 μm.

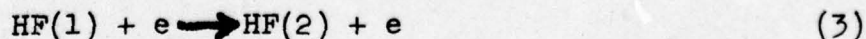
The primary activation energy is supplied by the discharge electrons via the process



The excited state decays to the ground state through the process



Some of the HF(1) molecules are excited into the next higher level via



Within each vibrational manifold the rotational sub-levels take on a distribution of their own, a low temperature Boltzmann profile since the rotational motion equilibrates rapidly with the translational motion. It can be shown that the threshold condition for the P-transitions is given by<sup>(1)</sup>

$$N_1 e^{\frac{2BJ}{kT_R}} > N_0 \quad (4)$$

where  $N_0, N_1$  are the population densities in the  $v = 0, 1$  manifolds,  $B$  the HF rotational constant and  $J$  the rotational quantum number. The above expression defines the so-called "partial inversion", a dynamic equilibrium of high vibrational and low rotational temperature.  $T_R$  is the rotational temperature and  $k$  the Boltzmann constant.

The two essential requirements for the attainment of laser threshold are a high electron collisional excitation rate and rapid rotational equilibration of HF at a low temperature.

It can be shown theoretically that for a rotational temperature of  $500^\circ\text{K}$  an electron density on the order of  $10^{13} \text{ cm}^{-3}$  is required to reach the theoretical threshold for laser gain.

The partial pressures for HF and He were chosen to optimize the achievable laser gain. According to published experimental observations<sup>(2,3)</sup> a partial HF pressure on the order of a few torrs appears to be optimum. At substantially higher pressures self-quenching of HF becomes excessive while at much lower pressures the density of active molecules is too low. The HF dilution in He must be on the order of 1:100. Otherwise electron attachment by HF reduces the electron current below the threshold level.

It can be shown that a self sustained discharge for the case of interest requires an average electron energy of nearly 4 eV, which is one order of magnitude higher than necessary for the vibrational excitation of HF and in the case of CW operation would lead to intolerable gas heating and arc formations. For this reason it is essential that the discharge be augmented by an injected electron beam which takes over the task of providing charge carriers by ionizing a large number of He atoms.

For externally controlled plasmas the applied sustainer field and hence the electron energy can be much lower than that necessary for self-sustaining discharges. In fact, the Townsend multiplication process in the plasma can be below threshold thus eliminating this breakdown mechanism.

To fulfill the second essential requirement for steady state laser gain, namely the maintenance of a low gas temperature, the plasma is confined to a channel of millimeter cross-section or less to increase the thermal diffusion to the confining walls. The sustainer discharge is formed across one of the narrow dimensions between an array of independent electrodes on one side and a titanium foil, which serves as a septum between the discharge vessel and the electron gun.

The narrow rectangular channel is built from slabs of sapphire and closed off at the top by a 0.0003" titanium foil. An array of 50 parallel copper-tungsten strips are embedded in a sapphire plate to form the base of the discharge channel. The side walls of the

waveguide are formed by the polished edges of two thin sapphire slabs. The total length of the waveguide is 8 cm. Brewster windows providing optical passage seal the channel at either end.

The auxiliary E-beam emanates from a heated filament which extends along the entire length of the discharge channel on the other side of the foil inside an evacuated glass dome. The electrons are accelerated towards the foil which they penetrate to enter the discharge plasma.

The present discharge vessel is operated in repetitively pulsed fashion, in order to introduce the thermal loading gradually. The duty cycle can then be increased towards CW operation. While the discharge vessel should eventually be operated as a sealed-off unit, the present system maintains a flow of active gases through the waveguide to circumvent the contamination problem occurring in sealed vessels.

During this reporting period most of the effort was directed towards the construction of the laser and auxiliary experimental apparatus. This work has been concluded recently and measurements of HF fluorescence have been carried out.

Since the radiative decay rate of HF(1) is rather small, a low noise detection system was assembled and carefully shielded from pickup signals to detect the characteristic HF fluorescence. Interference filters were used to separate the signal from the discharge continuum. From the fluorescence intensity it appears that the present degree of excitation in the HF/He mixture is not sufficient for level inversion. However, the degree of excitation can be

enhanced if hydrogen gas is added to the mixture to sensitize the pumping process via  $H_2$  to HF V-V exchanges. For the remainder of this contract HF/ $H_2$ /diluent mixtures will be employed with the goal of demonstrating laser gain

## II. BACKGROUND AND ANALYSIS

During the last several years the development of HF(DF) lasers has progressed to the point that this technology may now be directed toward applications in pointing and tracking, optical radar, communication and general surveillance. Those applications call for highly stable laser sources as local and/or master oscillators in addition to high power laser amplifiers.

The present chemical mixing HF(DF) lasers employ a flowing gas mix to provide vibrational activation of HF(DF) via an exothermic chemical reaction between hydrogen and fluoride. Fresh reactants are supplied continuously and exhausted by vacuum pumps after combustion. Not only are those systems bulky but their inherent frequency and amplitude stability are severely impaired by variations in the gas flow, the local combustion processes as well as by acoustic and mechanical perturbations from the mechanical pumps.

Attempts have been made to reduce these perturbances but the passive stability of such devices has up to now been limited to values exceeding 1 MHz.<sup>(4)</sup> Somewhat better stabilities have been obtained by locking the laser to an external passive standard such as a Fabry-Perot resonator;<sup>(5)</sup> however, active stabilization methods are limited by the bandwidth and gain of the locking loop circuit, and introduce a considerable system complication.

The ultimate aim of the present program is the development of a low power HF laser which exhibits a passive stability comparable to that of  $\text{CO}_2$  lasers since the purely electrical pumping mechanisms can be carried out in a sealed-off plasma vessel which leaves the optical resonator essentially unperturbed. Although the electrical pumping mechanism is different from that of conventional chemical HF lasers, the position of the spectral emission lines are identical.

The feasibility of a purely electrical HF laser has been demonstrated previously for pulsed excitation using an E-beam stabilized, transverse discharge in a relatively large active volume.<sup>(2,3)</sup> Subsequently, it was recognized at AIL that continuous operation of such a system would be possible if the active volume was scaled down to a channel of submillimeter cross-section. Because of the high thermal dissipation of such a structure, a low gas temperature can be maintained in steady state operation despite intense plasma heating which may exceed  $1 \text{ kW/cm}^3$  for the case of interest. It should be noted that the thermal diffusion rate increases with the inverse square of the channel diameter while the thermal dissipation density in the plasma remains constant. It can be shown that for the gas mix of interest and for a submillimeter channel diameter the temperature rise can be held to less than  $100^\circ\text{C}$ .

The attainment of laser gain in the HF/He discharge depends on the following elementary interactions:

1. Vibrational excitation of HF by electron impact (e-V)
2. Collisional relaxation of the vibrational mode (V-T)
3. Equilibration of the rotational states of each vibrational manifold at a low temperature by rapid interaction with the translational motion of the constituent gas particles (R-T)
4. Vibrational exchange reactions, intra- and intermode (V-V)

What makes level inversion possible is the large difference in these various reaction rates<sup>(6)</sup>. Rotational equilibration in an HF gas occurs at a rate about ten times the hard shell collision rate while transfer of HF rotational energy to the helium translational motion takes place approximately once every hard shell collision with He atoms. The  $\text{HF}(1) + \text{HF}(0) \longrightarrow 2 \text{HF}(0)$  deactivation proceeds at 1/100 the hard shell collision rate and  $\text{HF}(1) + \text{He} \longrightarrow \text{HF}(0) + \text{He}$  occurs on every  $10^5$ th collision. There is good reason therefore to assume that the rotational motion of HF is equilibrated at the gas temperature while the vibrational temperature excitation corresponds to a distribution temperature closer to that of the electrons. Inversion between levels  $(v = 1, J-1)$   $(v = 0, J)$  requires that<sup>(1)</sup>

$$\frac{\sum_J N_{1,J}}{\sum_{J'} N_{0,J'}} \exp \left( 2J \cdot \frac{hcB}{kT_R} \right) > 1 \quad (5)$$

where the vibronic states are labeled in the conventional way; h, c, k are the familiar universal constants, B is the rotational energy constant of HF and  $T_R$  the so-called rotational temperature assumed to be equal to the translational temperature T of the gas. Equation (5) shows that there can be a population inversion for P-transitions



even if the total number of HF molecules in the upper vibrational manifold is less than that in the lower one. This condition is called "partial inversion." If the degree of excitation is not too high one can approximate

$$\frac{\sum_J N_{1,J}}{\sum_{J'} N_{0,J'}} = \frac{\sigma j \tau}{e} \quad (6)$$

where  $\sigma$  is the cross-section for the e-V process,  $\tau$  is the time constant for the V-T process,  $j$  is the electric current density and  $e$  the electron charge.

Unfortunately, the cross-section  $\sigma$  for electron impact excitation is relatively small,  $\sim 3 \times 10^{-17} \text{ cm}^2$ <sup>(2)</sup> and the V-T relaxation quite rapid, therefore it is necessary to provide a current density of  $\approx 10 \text{ A/cm}^2$  in the plasma to attain level inversion, corresponding to an electron density of  $\approx 10^{13}/\text{cm}^3$ .

In self-sustained discharges the electron energy must be sufficiently high to produce a rate of ionization equal to the rate at which electrons disappear from the plasma. Considering only the dominant volume recombination for a 300 torr He, 5 torr HF gas for an electron density of  $N = 10^{13} \text{ cm}^{-3}$ , and estimating a recombination factor of  $\beta = 10^{-7}$ , a loss rate of  $\frac{dN}{dt} = \beta N^2 = 10^{19} \text{ ion pairs/cm}^3 \text{ sec}$  is calculated. Therefore the loss rate per electron is  $10^6 \text{ sec}^{-1}$ . To replenish those lost charge carriers in a self-sustained discharge the average electron energy must be about 3.7 eV, assuming Boltzmann distribution.<sup>(7)</sup> Since the electron impact excitation of

HF has a threshold energy of 0.45 eV, a plasma with an average electron energy of 3.7 eV is badly mismatched to the e-V pumping mechanisms. At such a high electron energy there would be an intolerable increase in gas temperature leading to arc formation. Also, at such high electron energies HF molecules dissociate at a high rate. If, however, the discharge is augmented by an injected beam of high energy electrons, the average electron energy can be reduced to a safe value of 1 eV or less while maintaining the high electron density of  $10^{13}/\text{cm}^3$ . Now the replacement of charge carriers is taken care of by the injected electrons through ionization of the He atoms while the discharge electrons need only sufficient energy to overcome the collisional losses.

It was recognized that the narrow gap discharge geometry offers an additional benefit in that it permits the use of a very thin foil since the unsupported foil area is a very narrow strip equal to the channel width such that the mechanical stress on the foil is small and the thermal conduction path short. There is less attenuation of the E-beam for a thin foil. Also, once the electrons have penetrated the foil they need relatively little energy to cross the narrow channel. Hence, the acceleration potential of the E-gun can be relatively low. Measurements for the case of a 0.0003" titanium foil and 50 kV acceleration potential, indicate that sufficient electrons penetrate into the plasma to lower the breakdown voltage perceptibly. With lower electron energies the ionization probability goes up.

Ionization by the injected electrons must balance the loss of charge carriers due to diffusion, recombination and attachment

processes. (The total electron loss rate has been estimated to be  $10^{19}/\text{cm}^2$ .) To provide an equal rate of ionization processes the injected electron beam must have a current density equal to

$$j' = \frac{10^{19}e}{p \cdot s} \quad (7)$$

where  $p$  is the pressure inside the plasma vessel in torr,  $s$  is the number of ion pairs generated by one injected electron per cm path length at a gas pressure of 1 torr, and  $e$  is the electron charge. Inserting  $s = 1$ ,  $p = 300$  we obtain  $j' = 5 \times 10^{-3} \text{ A/cm}^2$ .

The energy loss of fast electrons in the titanium foil is roughly approximated by the formula<sup>(8)</sup>

$$\frac{\Delta E}{\Delta x} = \frac{0.17}{E} \ln(6600 \cdot E) \quad (8)$$

where  $E$  is the incident electron energy in MeV and  $\Delta x$  the foil depth in cm. For example, if  $E = 5.0 \times 10^{-2} \text{ MeV}$  (50 kV) and  $dx = 7.5 \times 10^{-4} \text{ cm}$  (0.0003") then the electrons suffer an energy loss of  $\approx 15 \text{ kV}$ . The power dissipated in the foil is very high,  $6 \times 10^4 \text{ W/cm}^3$  for a current density of  $5 \text{ ma/cm}^2$ . But due to the short conduction path in the foil, the temperature rise is moderate. Ohmic heating in the foil by the discharge current is negligible. The foil is attached to a cooled alumina substrate with a narrow slit over the channel area to provide passage for the high energy electrons. In steady state operation the temperature profile across the unsupported strip of foil is parabolic with a peak temperature rise at the center given by:

$$\Delta T = \frac{q \left(\frac{1}{2} a\right)^2}{2k} \quad (9)$$

where  $q$  is the density of dissipated power,  $a$  the width of the exposed foil strip and  $k$  the coefficient of thermal conduction for titanium. Inserting  $q = 6 \times 10^4 \text{ W/cm}^2$ ,  $a = 1/30 \text{ cm}$ , and  $k = 0.16 \text{ W/cm}^\circ\text{C}$ , a peak temperature rise of  $\approx 50^\circ\text{C}$  is calculated at the center of the foil. If the copper-tungsten electrode array is used as the cathode and the helium gas pressure is 300 torr, the cathode fall voltage of a self-sustained discharge is  $\approx 150$  volts and its thickness  $1/400 \text{ cm}$ , a small fraction of the total gap width (see Reference 7). In the presence of the injected E-beam, the cathode fall voltage assumes a lower value. To obtain the total voltage drop across the entire discharge, one must add the voltage contributed by the drift field, 300 V/cm for the plasma of interest, or 10 volts for a  $1/30 \text{ cm}$  discharge length. The anode and cathode surfaces which form two opposing walls of the discharge channel must be efficiently cooled to avoid additional heating of the gas. The cathode temperature is not easily calculated since the power dissipation associated with the electron injection process and heating from the cathode fall layers are modified in the presence of an injected E-beam. In any case, it is apparent that the dissipation in the cathode fall is very high. But the heat generated is practically at the cathode surface and hence removed very efficiently. The heat which is generated throughout the channel volume will be conducted to the sapphire sidewalls which are at a much lower temperature than the electrode walls. For a drift field of 300 V/cm and a current density of  $5 \text{ A/cm}^2$ , the power dissipation is  $1.5 \text{ kW/cm}^2$ . The gas temperature profile which develops across the waveguide is parabolic as in the case

of the foil and the peak temperature rise is also given by equation (9). For  $q = 1.5 \times 10^3 \text{ W/cm}^3$  and for helium ( $k = 0.002 \text{ W/cm}^\circ\text{C}$ ) a temperature rise of about  $100^\circ\text{C}$  at the center of the channel is calculated.

It has been assumed that the relaxation within each system of rotational levels is governed by the collisional R-T energy transfer to the abundant helium atoms; the rotational level population assumes a Boltzmann distribution of temperature  $T_R$  equal to the gas temperature  $T$ . From equation (4), it follows that the laser gain can only be achieved for any P-transition if  $T_R (=T)$  is sufficiently small. Therefore adequate cooling of the discharge gas by thermal diffusion to the channel walls is of critical importance. Given the high heating rate in the plasma discharge and the low thermal conductivity of the gases, calculations indicate that the thermal conduction path must be less than 1 millimeter to hold the rise in gas to a tolerable value of about  $100^\circ$ .

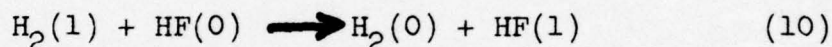
It should be noted that the HF-EDL must be operated as a waveguide resonator since a free Gaussian beam would not clear the channel. Waveguide resonators have been routinely used in  $\text{CO}_2$  lasers and represent an area of existing technology. The optical waveguide loss scales with the ratio of capillary diameter to wavelength,  $d/\lambda$ , and is estimated at  $0.001/\text{cm}$  for a  $1/3 \times 1/3 \text{ mm}$  channel and  $\lambda = 2.9 \text{ }\mu\text{m}$ . (9)

Waveguide lasers have been operated with a variety of optical configurations. In the simplest case, flat mirrors are attached to both channel openings. For this application, another arrangement is preferred in which two spherical reflectors are placed at some distance from the channel such that the radiation emerging from either opening is focused back into the channel. At the channel openings there will be a certain amount of coupling loss in transforming the free space Gaussian wave shape into a guided wave. Based on  $\text{CO}_2$  laser measurement data, this coupling loss is relatively small ( $\approx 0.01$  at each end) due to the excellent match of the free space's Gaussian and the guided wave's Bessel beam profiles. (9)

The important role played by V-V collisional transfer processes is treated below. These processes are of crucial importance in CO lasers which in principle are similar to the electrical HF laser system. For CO lasers the V-V relaxation rates are much faster than the V-T processes and, under suitable conditions, a gas may relax to a state of vibrational quasiequilibrium before V-T processes become important. The collisional V-V exchange may occur between different molecular species (intermode exchange) or between different vibrational levels of the same species (intramode exchange). For an anharmonic oscillator the intramode exchange may be the controlling mechanism in the relaxation process. In an analysis by Treanor, et al<sup>(10)</sup> it was shown that V-V exchange collisions create a non-Boltzmann distribution in a relaxing gas of anharmonic

oscillators. This distribution may actually exhibit a total population inversion among the higher vibrational level. Caledonia and Center<sup>(11)</sup> have refined the model and demonstrated that V-T processes prevent a large inversion between upper vibrational levels which might otherwise occur as a result of intramode V-V exchanges.

Intermode V-V transfer plays an important role in this case also since the pumping process for an electrical HF laser is sensitized by addition of hydrogen gas. The H<sub>2</sub> is excited by electron impact (just as HF is) into the v = 1 state and transfers this excitation efficiently to HF:



Theoretically, the reaction of equation (10) represents a much more efficient pumping mechanism than the reaction of equation (1) because H<sub>2</sub>(1) exhibits a longer lifetime than HF(1) while the cross-sections for electron collision pumping are about equal for HF and H<sub>2</sub> molecules. Consequently, the degree of excitation will be much higher for H<sub>2</sub> than for HF. The remaining question is whether the H<sub>2</sub> → HF V-V transfer is sufficiently rapid to overcome HF self quenchings. Noting that the thermal energy of the gas constituents is much smaller than their vibrational quantum energies, one obtains the expression

$$\frac{N_1}{N_{0/\text{HF}}} = \frac{N_1}{N_{0/\text{H}_2}} \exp\left(\frac{\Delta E}{kT}\right) \cdot \frac{1}{1 + \frac{\tau_{\text{V-V}}}{\tau_{\text{V-T}}}} \quad (11)$$

from Reference (11).

Where  $\Delta E$  is the difference in vibrational quantum energy of HF and  $H_2$ ,  $T$  the gas temperature, and  $\tau_{V-V}$ ,  $\tau_{V-T}$  are the time constants for V-V transfer and HF self quenching, respectively. The exponential factor in equation (11) is positive due to the exothermic character of reaction (10) (for  $T = 300$ ,  $\Delta E/kT \approx 1$ ), and the quotient factor in (11) illustrates that for efficient coupling the V-V process must occur at a faster rate than HF self quenching. The above time constants can be calculated from the relations:

$$\tau_{V-V} = \frac{1}{k_{V-V} \cdot p_{H_2}}, \quad \tau_{V-T} = \frac{1}{k_{V-T} \cdot p_{HF}} \quad (11a)$$

where  $k_{V-V}$ ,  $k_{V-T}$  are the respective rate constants and  $p_{H_2}$ ,  $p_{HF}$  the partial pressures. Since  $k_{V-V} \approx k_{V-T}$ ;  $\frac{\tau_{V-V}}{\tau_{V-T}} = \frac{p_{HF}}{p_{H_2}}$ , i.e., the partial pressure of  $H_2$  must exceed that of HF by a large margin for efficient V-V transfer.

The importance of V-V transfer has been verified by reported experimental data.<sup>(2)</sup> Laser intensity for a HF/ $H_2$ /diluent mixture was 1 to 2 orders of magnitude higher than that for HF/diluent mixtures. Similarly, when  $H_2$  was replaced by  $D_2$  the laser intensity fell by one order of magnitude.

To estimate the laser gain  $g$ , the saturation intensity  $S$ , and the optical power  $P$ , the following relationships can be employed:

$$g = \sigma_0 \cdot D \quad (12)$$

$$S = \frac{h\lambda}{\sigma_0 c} \cdot Y \quad (13)$$

$$P = \nu \cdot g \cdot S \quad (14)$$



where  $\sigma_0 = \frac{\lambda^2 A}{8\pi\Delta\nu}$  is the cross-section for stimulated emission and the parameter D for the P(J) transition is given by:

$$D = (2J+1) \frac{hcB}{kT} \left[ N_{v+1} \exp \left\{ -\frac{hcB}{kT} J (J-1) \right\} - N_v \exp \left\{ -\frac{hcB}{kT} J (J+1) \right\} \right] \quad (15)$$

$\lambda$  is the optical wavelength,  $\pi\nu$  the linewidth,  $\gamma$  the decay rate of the upper laser level,  $V$  the active volume and A the Einstein coefficient for the transition.

For the R<sub>1</sub>(11) transition with a partial HF pressure of 0.8 torr, an average gas temperature of 400°K,  $\lambda = 3 \times 10^{-4}$  cm,  $A = 100 \text{ sec}^{-1}$ , <sup>(12)</sup>  $\Delta\nu = 300 \text{ MHz}$  <sup>(4)</sup>, assuming a ratio of  $N_2:N_1:N_0 = 1:3:15$  for the population densities in the  $v = 2,1,0$  manifolds of HF and inserting  $\gamma \sim 10^5 \text{ sec}^{-1}$  <sup>(2)</sup>, one finds  $g = 0.004 \text{ cm}^{-1}$  and  $S = 300 \text{ W/cm}^2$ . For a channel volume of  $\frac{1}{30} \times \frac{1}{30} \times 10 = \frac{1}{90} \text{ cm}^3$  the estimated output power is then equal to 1 mW of which more than half can be extracted as laser output.

### III. LASER DEVICE AND EXPERIMENTAL EFFORT

Most of the work during this reporting period was devoted to the construction and testing of the experimental apparatus consisting of the HF laser head, the power supplies, the gas handling equipment and the fluorescence radiometer. A repetitively pulsed discharge is operated in a flowing HF/He gas mixture. The laser head is connected to a metered gas supply and mixing manifold and the spent gases are pumped from the laser head and removed from the laboratory by a special exhaust system.

In assembling the HF laser several time-consuming obstacles had to be overcome such as the attainment of vacuum tight seals between a variety of dissimilar materials, the elimination of E-gun arcing and the mounting of the 0.0003" foil. The need for special corrosion resistant materials complicated the construction of the laser head. Standard electron tube processing techniques were used wherever possible in fabricating the E-gun assembly.

By demonstrating the operation of an E-beam stabilized electric discharge in an HF-He gas and observing HF fluorescence we have accomplished the first important step towards demonstration of a waveguide HF-EDL. Figure 1 shows a schematic view of the HF laser head. The active gases are admitted into the discharge area through a copper baseplate. Attached to it is a Kel-F shell which encloses the actual discharge assembly consisting of the copper-tungsten electrode array embedded into a sapphire block which forms the base of the waveguide channel. Two sapphire slabs are placed on top of the base to form a rectangular channel. For the purpose of this proof of principle phase a 1 x 1 mm channel is used to simplify construction. The bottom and sidewalls are polished to provide an optical waveguide. The titanium foil which closes off the channel and separates it from the evacuated E-gun assembly is attached to a slotted alumina substrate which in turn is mounted to a stainless steel frame. The steel frame rests on top of the Kel-F shell and the shell is sealed off with an O-ring. Two sapphire Brewster windows provide an optical passage through the sealed shell. The sustainer discharge is struck between the electrode array and the titanium foil. A thin copper ribbon provides electrical contact to the foil.

Individual sustainer discharges are formed between each array element and the titanium foil in TEA laser fashion. The glass dome which holds the E-gun filament is attached to the top of the steel frame such that the filament lines up with the discharge channel. Figures 2 and 3 show the laser head in successive stages of assembly.

The E-gun acceleration potential is applied to the heated filament as a negative pulse. In the present assembly, the acceleration potential can be adjusted between zero and -50 kV and the foil thickness is 0.0003". At a potential of 50 kV, the penetrating electrons emerge from the foil with an average energy of 35 kV, more than enough energy to traverse the channel even at atmospheric fill pressures.

It is apparent from the above considerations that the two key requirements in attaining partial level inversion for certain HF vibronic transitions are: (1) a high electron density, and (2) a low rotational temperature for the HF molecules. During the current program, the stated goal is to initially excite the HF laser in pulsed fashion and then to increase the pulse rate and pulse width gradually towards higher duty cycles (or CW) operation so that the thermal loading is introduced in a controlled manner.

The electrical schematic in Figure 1 illustrates the circuitry for sustainer and E-beam pulses which are triggered to appear simultaneously at the discharge vessel.

The capacitors C are charged through individual resistors R from a common supply which is also connected to the foil. Upon the trigger command a hydrogen thyatron shorts the common point "A" to ground causing the capacitor voltage to appear across the discharge gap.

Some discharge data are shown in Figure 4 for illustrative purposes. The top two oscillograph traces represent the electrical potential at the foil as a function of time. The scope is triggered together with the thyatron and the full charge voltage is measured at the foil. When the thyatron is fired it represents only a small impedance and the foil is connected to ground through this small impedance and an inductive element. Consequently, the potential of the foil drops rapidly to a very low value. Simultaneously, the 50 capacitors C discharge through their individual resistors with a time constant of  $RC = 2.2 \mu\text{sec}$ . When the thyatron current reaches a critical low value, its impedance is rapidly switched back to a high value, and the recharging of the capacitors C begins raising the potential at the foil slowly to its previous high value (recharging not perceptible on the displayed time scale). In example A of Figure 4 the charge voltage was below the value for breakdown such that no discharge across the gap could take place.

In example B of Figure 4 the gap array is substantially over-volted and breakdown occurs upon thyatron firing. The discharge current across the gap array superimposes a positive voltage component at the foil driving its potential up to a value of about  $1/2$  the initial voltage. Eventually the potential difference across the gap falls below a critical value, the discharge is switched off and the recharging commences.

The minimum breakdown voltage vs helium gas pressure for repetitive pulsing at 5 pps is given in Figure 4C. Single shot discharges required much higher voltages. One may try to explain this

by assuming that the charge carriers remain in the volume from one pulse to the next for repetitive pulsing. However, at a volume flow of  $10\text{-}20\text{ cm}^3\text{ sec}^{-1}$  the channel is refilled more than 100 times per second. While it is difficult to see how volume pre-ionization can be maintained it is possible that charge carriers attach themselves to the nonmetallic parts of channel walls for sufficiently long periods to effect subsequent discharge pulses. Other explanations may be sought in the processes occurring on the electrode surfaces, which will be at a higher temperature for repetitive pulsing.

After the thyatron has been fired another trigger signal initiates the generation of the E-gun pulse which is stepped up to a maximum of -50 kV. The filament voltage is applied through an isolation transformer.

Figure 5 shows a photographic overview of the experimental setup consisting of the electronics, laser head, evacuation equipment, gas metering manifold and fluorescence radiometer.

Since HF is corrosive, special care had to be taken in assembling the gas handling equipment. Although the final aim of this development is to seal the active gases inside the laser, a slight gas flow is maintained in the present system to avoid contamination problems during the proof-of-principle effort. The active gases are released from storage bottles at precisely controlled rates and mixed upstream of the laser vessel. After passage through the vessel the gases are pumped off by a mechanical vacuum pump and safely exhausted from the building.

The study of level inversion conventionally involves the observation of fluorescence from the levels in question. At the threshold of level inversion a nonlinear increase in fluorescence intensity is observed which is the best indication of optical gain short of laser oscillation. However even below that threshold the fluorescence intensity gives a good indication of the degree of excitation. Only a portion of the radiation generated in the plasma channel appears at the capillary openings, but that portion is peaked in the forward direction. The emerging radiation is then focused onto a photodetector, an InSb PV device of 0.005" diameter placed inside a dewar shown in Figure 6. The photodetector equivalent circuit and the amplifier circuit are shown in Figure 7. The bandwidth of this system is less than 1 MHz, just about wide enough to resolve the signal pulses. The signal level at the first amplifier output,  $V_p$  is equal to  $i_s R_f$  where  $i_s$  is the photocurrent at the amplifier input, given by the detector current responsivity  $S$  times the intercepted optical power. Since  $S = 1.5$  amps/watt and  $R_f = 68$  kilohms, the voltage at the output of the first amplifier equals 1 volt for  $10^{-5}$  W of intercepted radiation at  $3 \mu\text{m}$ . The second amplifier stage provides a 10 dB voltage gain, such that the overall system sensitivity is 1 volt/1  $\mu\text{W}$ .

The noise sources to be considered are: (1) background radiation, (2) detector dark current, and (3) amplifier noise.

To suppress the discharge continuum narrow bandwidth interference filters of 0.2 and 0.02  $\mu\text{m}$  halfwidth are placed in front of the dewar

window. An  $\text{As}_2\text{S}_3$  lens of 0.300" focal length and 0.4" diameter is mounted inside the dewar, close to the photodetector and a cylindrical shroud acting as a cold baffle blocks out all background radiation except that entering through the lens. Of the background radiation entering the lens only a small portion falls on the detector. To estimate the magnitude of the intercepted background radiation we assume a background temperature of  $300^\circ\text{K}$  and an emissivity of 0.5. The background radiance then is  $W_\lambda = 2 \times 10^{-6} \left[ \frac{\text{W}}{\text{cm}^2 \text{sterad } \mu\text{m}} \right]$  and the radiation reaching the detector is given by  $W_\lambda \cdot \Delta\lambda \cdot \Delta\Omega \cdot A_2$ , where  $\Delta\lambda$  is the bandwidth of the filter,  $\Delta\Omega$  the solid angle intercepted by the internal lens, and  $A_2$  the clear lens area. For  $\Delta\lambda = 0.2$ ;  $\Delta\Omega = (1/60)^2$  sterad and  $A_2 = 0.7 \text{ cm}^2$  the background radiation reaching the detector is approximately  $1 \times 10^{-10} \text{ W}$ .

The detector noise is given by  $\text{NEP} = \frac{A \sqrt{B}}{D^*}$  where A is the detector area and B the receiver bandwidth. Inserting the values  $A = 1.26 \times 10^{-4} \text{ cm}^2$ ,  $B = 1 \times 10^6$ ,  $D^* = 3.6 \times 10^{11} \left[ \frac{\text{cm Hz}^{1/2}}{\text{W}} \right]$  the calculated NEP is  $3 \times 10^{-11} \text{ W}$ .

The largest noise contribution comes from the first amplifier, leading to a 2 mV peak to peak average fluctuation at the oscilloscope which corresponds to an NEP of  $2 \times 10^{-9} \text{ W}$ . A difficult experimental problem is the RF noise due to pickup signals. To reduce the pickup the amplifier is operated with batteries in a small enclosed package that is attached directly to the detector dewar to keep the transmission path from the detector as short as possible; the discharge vessel and pulse generating networks are enclosed with copper screening.

The first fluorescence measurements are illustrated in Figure 8. Oscillographs (A) and (B) show the photo signal obtained with the receiver shown in Figure 6. Figures 8A and 8B correspond to discharges in pure helium and HE/HF, respectively. Note the long tail in trace (B) which demonstrates that the lifetime of the vibrationally excited state of HF exceeds the length of the discharge pulse. A narrow interference filter (Figure 8C) was used in both cases to block out the spectrally broad emission of the discharge plasma. When the HF fluorescence signal (B) is plotted on a semi-log scale (Figure 8D) one notes that the initial and fastest decay process occurs with a 3  $\mu$ sec time constant. Since the HF partial pressure was 5 torr, this value is in good agreement with the vibrational decay rate of  $6 \times 10^{+4} \text{ sec}^{-1} \text{ torr}^{-1}$  at 300°K reported by Hinchey<sup>(6)</sup>.

For a narrow discharge channel one must consider the role of wall collisions on the HF(1) lifetime. Diffusion of the HF molecules to the wall, seen as a random walk process, occurs with the time constant

$$\tau_D = \frac{a^2}{\lambda \cdot \bar{c}} \quad (16)$$

where  $a$  is the channel diameter,  $\lambda$  the mean free path of HF and  $\bar{c}$  the average velocity of HF molecules in the gas mixture. Considering a 300 torr He, 5 torr HF gas the mfp of HF is mainly determined by collision with He atoms;  $\lambda = 5 \times 10^{-5}$  cm. At 300°K the value for  $\bar{c} = 5.6 \times 10^{-4}$  cm/sec. Inserting these values and  $a = 0.1$  cm into equation (16) we get  $\tau_D = 3.6$  msec which is three orders of magnitude larger than the measured HF(1) quenching period.



A rough estimate of the degree of vibrational excitation can be obtained from the height of the photo signal, about 20 mV peak, which corresponds to a peak value of 20 mW optical power absorbed by the small InSb detector. A 5 torr partial HF pressure corresponds to a molecular density of  $N_0 = 1.8 \times 10^{17}/\text{cm}^2$ . Assume that a fraction  $\epsilon N_0$  is excited into the  $v = 1$  level, Boltzmann-distributed over all rotational sub-levels. The product of that distribution function with the normalized spectral transmission profile of the radiometer's interference filter yields the value 0.1. The weighted fluorescence power is then equal to  $0.1 \epsilon \cdot h\nu \cdot V \cdot \frac{1}{\tau_{\text{rad}}}$  where  $\tau_{\text{rad}}$  is the radiative lifetime of HF(1) and  $V$  the discharge volume =  $0.08 \text{ cm}^3$ . Of this only a fraction  $c_g$  is guided through the channel and transmitted out of the vessel, and only 1 percent again is absorbed by the detector. Since the absorbed signal had a peak power of 20 nW one calculates for the product  $\epsilon c_g \sim 2 \times 10^{-4}$ .

In view of the uncertainty of the value of  $c_g$  any estimate of the degree of excitation is unreliable at this point. But it appears that the present degree of excitation is not sufficient for level inversion. However, the degree of excitation can be enhanced by adding  $\text{H}_2$  to the mix which sensitized the pumping process via  $\text{H}_2$  to HF V-V exchanges. For the remainder of this contract we will concentrate on HF/ $\text{H}_2$ /diluent mixtures with the goal of demonstrating laser gain. Upon completion of this report it was discovered that the high current portion of the discharge pulse is only 1  $\mu\text{sec}$  long, even though the RC time constant for the anode voltage is 2.2  $\mu\text{s}$ . It is suspected that stray capacitances and inductances prevent the cathode from reaching ground potential rapidly enough such that the gap voltage is much smaller than assumed for most of the pulse period.

In any event, a 1  $\mu$ sec pulse duration is one order of magnitude smaller than the typical lifetime of the excited levels. Therefore, the population density in those levels is far below the asymptotic maximum.

Changes in the circuitry will have to be made to lengthen the discharge pulse adequately. A substantial increase in excited level population is expected from this measure.

## SUMMARY

The aim of this program is the development of a purely electric HF waveguide laser. Such a device is desirable for application in pointing and tracking, optical radar, communication, and general surveillance.

The HF vibrational motion is excited by inelastic electron collisions in an HF/diluent discharge plasma. Level inversion requires a high degree of vibrational excitation and an equilibration of the rotational sub-levels within each vibrational manifold at a low temperature by rapid R-T transfer to the diluent atoms.

The plasma is generated by a transverse discharge inside a 1 mm x 1 mm rectangular channel; an auxiliary E-beam is injected into the plasma channel to obtain a high discharge current density with minimum plasma heating.

In this way one not only avoids the formation of arcs but also eases the cooling problem. For the attainment of level inversion in steady state operation, thermal dissipation in the plasma channel is of crucial importance. The narrow discharge dimensions were chosen for efficient thermal conduction to the confining walls.

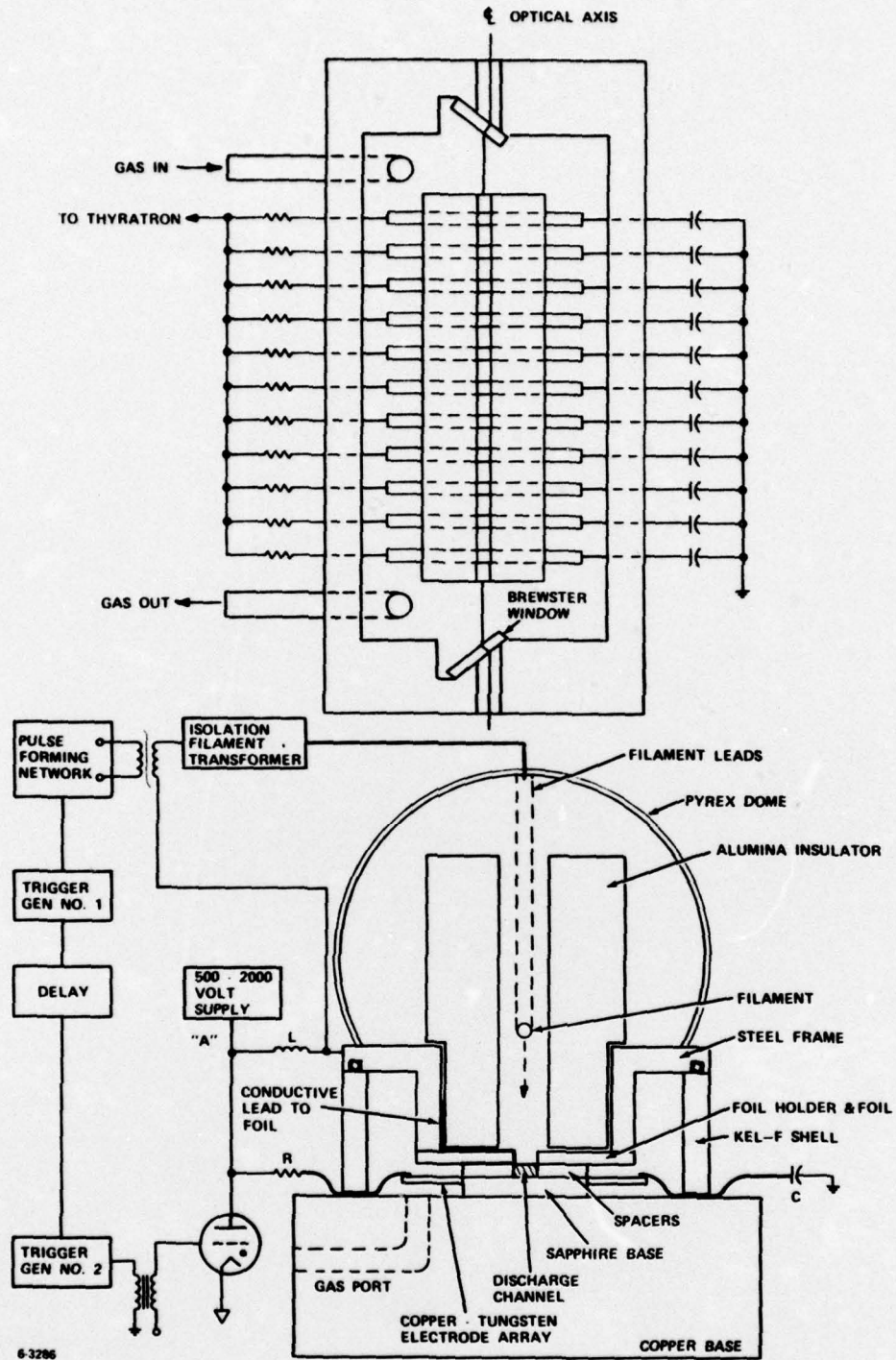
Pulsed high current discharges were obtained in gas mixtures varying from 150 to 650 torr total pressure at HF dilution ratios of  $\approx$  1:100 and the fluorescence from the excited vibrational levels were measured.

The observed fluorescence intensity suggests that the present degree of excitation is insufficient for laser gain. However, the degree of excitation can be significantly enhanced if  $H_2$  gas is added to the mix, to sensitize the pumping process via  $H_2 \rightarrow HF$  V-V transfer. For the remainder of this contract work will be concentrated on HF/ $H_2$ /diluent mixtures with the goal of demonstrating laser gain.

In addition, it was found that the high current portion of the discharge pulse was far too short (1  $\mu$ sec) for optimum excitation due to stray capacitances and inductances near the discharge channel. A substantial increase in excited level population can be expected when the discharge pulse will be sufficiently stretched.

## REFERENCES

1. J.C. Polanyi, Appl. Optics Suppl. on Chemical Lasers, pp 109-127, 1965.
2. S.R. Byron, et al, Final Report on N00014-72-C-0430 and Appl. Phys. Letter 23, pp 565-567, 15 Nov. 1973.
3. R.M. Osgood and D.L. Mooney, Appl. Phys. Lett. 26, pp 201-204, 15 Feb. 1975.
4. J.J. Hinchin and R.J. Freiberg, Appl. Optics 15, pp 459-461, Feb. 1976.
5. T. Thomson, TRW, private communication.
6. J.J. Hinchin and R.H. Hobbs, J. of Chem. Phys. 65, pp 2732-2739, 1 Oct. 1976.
7. A.V. Engel, "Ionized Gases," Oxford Press, 1965.
8. Hd. d. Physik, Vol. XXXIV, Springer, pp 55-138.
9. J.J. Degnan and D.R. Hall, IEEE of Quantum Electronics QE-9, pp 901-910, Sept. 1973.
10. C.E. Treanor, et al, J. of Chem. Phys. 48, pp 1798-1807, 15 Feb. 1968.
11. G.E. Caledonia and R.F. Center, J. of Chem. Phys. 55, pp 552-561, 15 July 1971.
12. J.K. Hancock and W.H. Green, J. of Chem. Phys. 57, pp 4515-4529, 1 Dec. 1972.



6-3286

Figure 1. Laser Head - Schematic

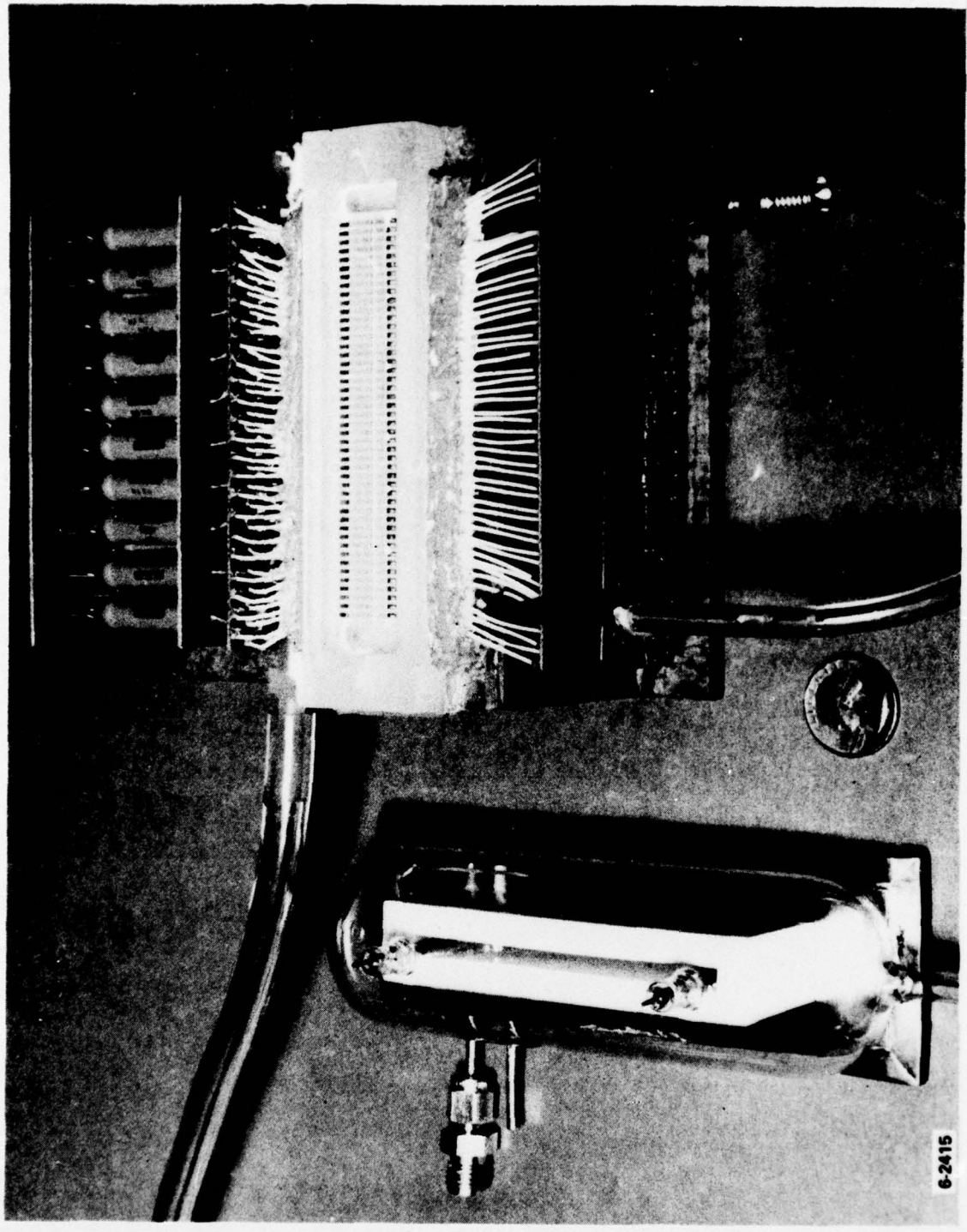
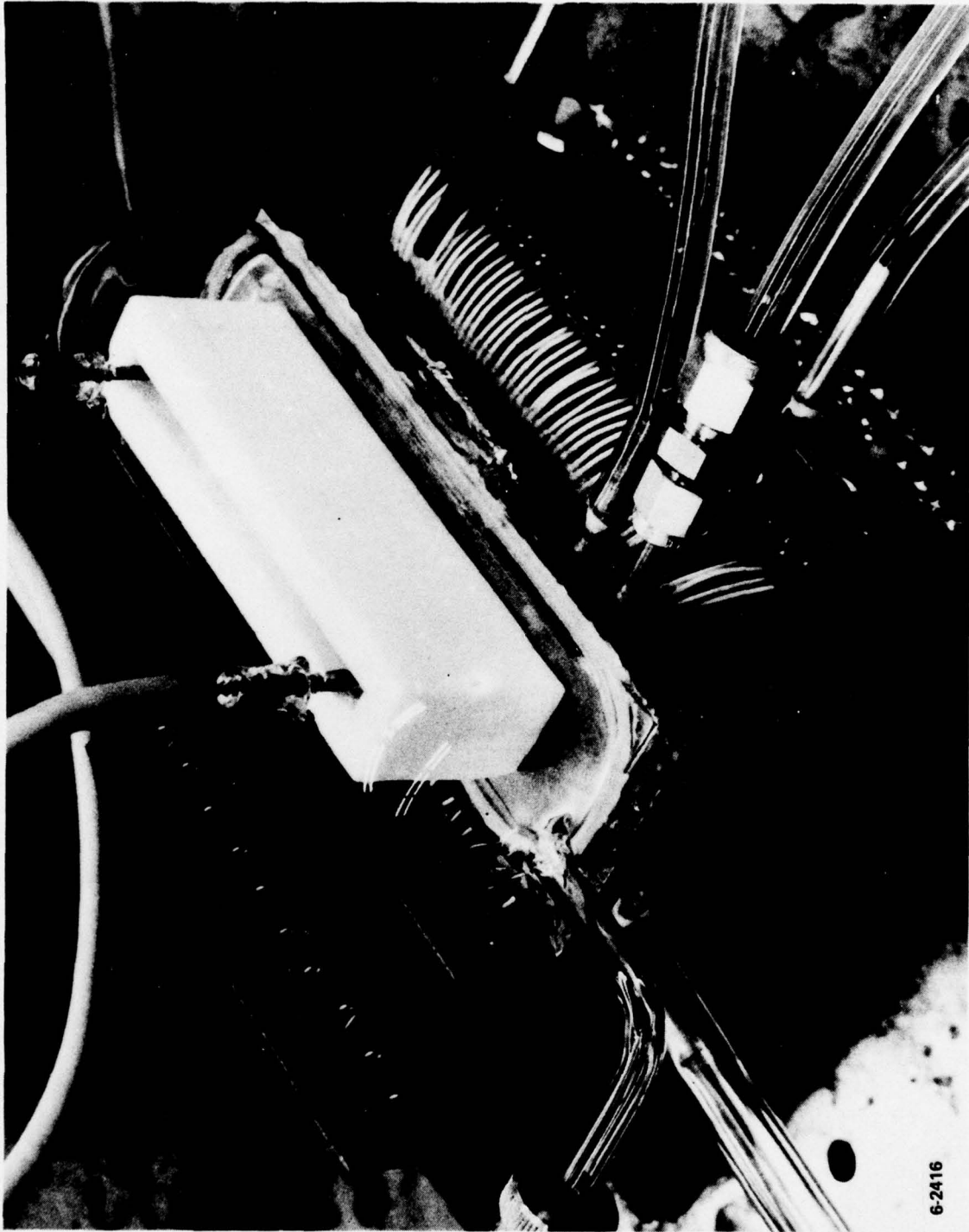


Figure 2. Laser Head - View No. 1



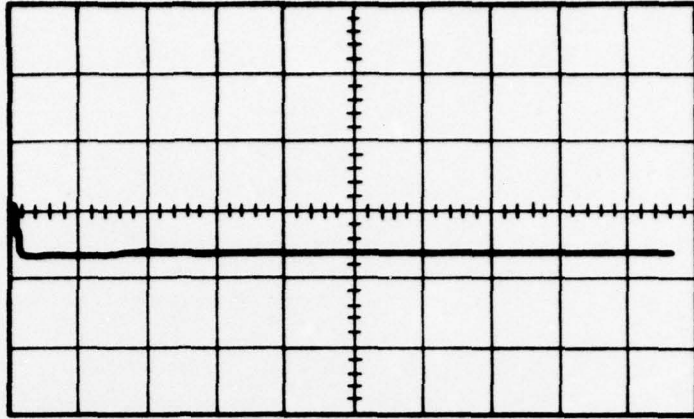
6-2416

Figure 3. Laser Head - View No. 2



d. POTENTIAL AT FOIL

$\left[ \frac{1 \text{ KV}}{\text{cm}} \right] \uparrow$

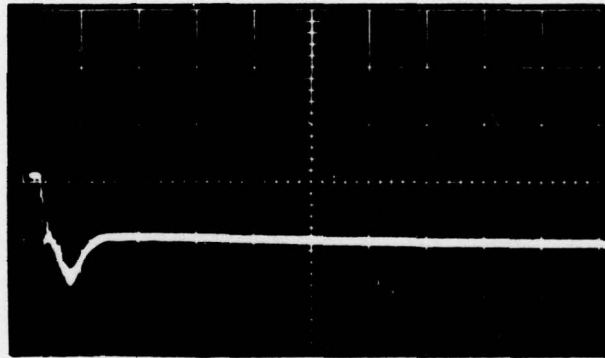


1  $\mu\text{s/cm}$

A. WITHOUT BREAKDOWN  $p = 150 \text{ Torr He}$ , CHARGE VOLTAGE 500 V

d. POTENTIAL AT FOIL

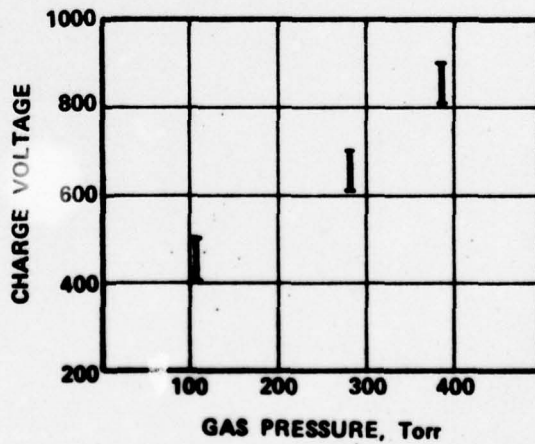
$\left[ 1 \text{ KV/cm} \right] \uparrow$



1  $\mu\text{s/cm}$

B. WITH BREAKDOWN  $p = 150 \text{ Torr He}$ , CHARGE VOLTAGE 2000 V

MINIMUM CHARGE VOLTAGE FOR BREAKDOWN



6-3287

Figure 4. Discharge Data

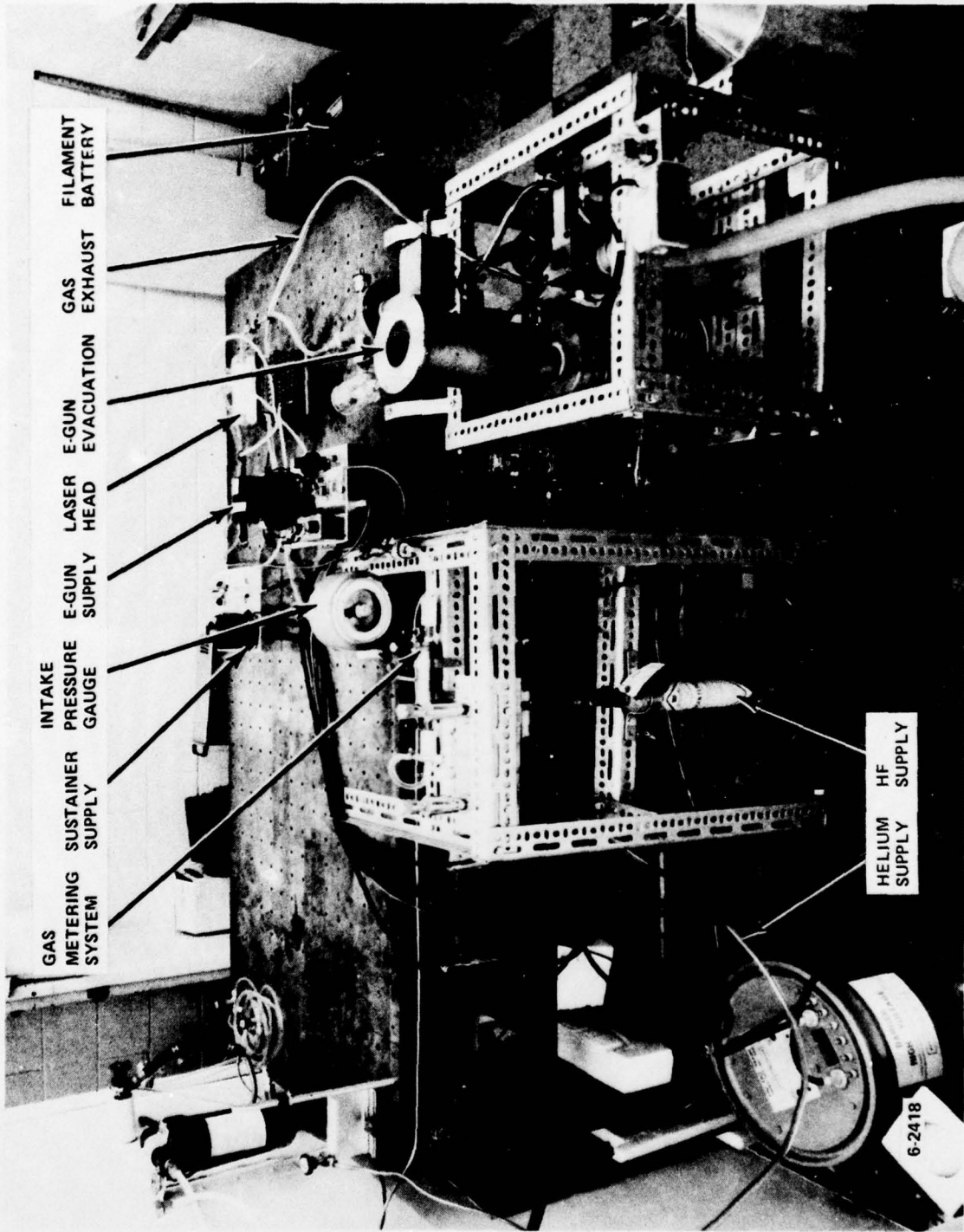


Figure 5. Experimental Set-Up

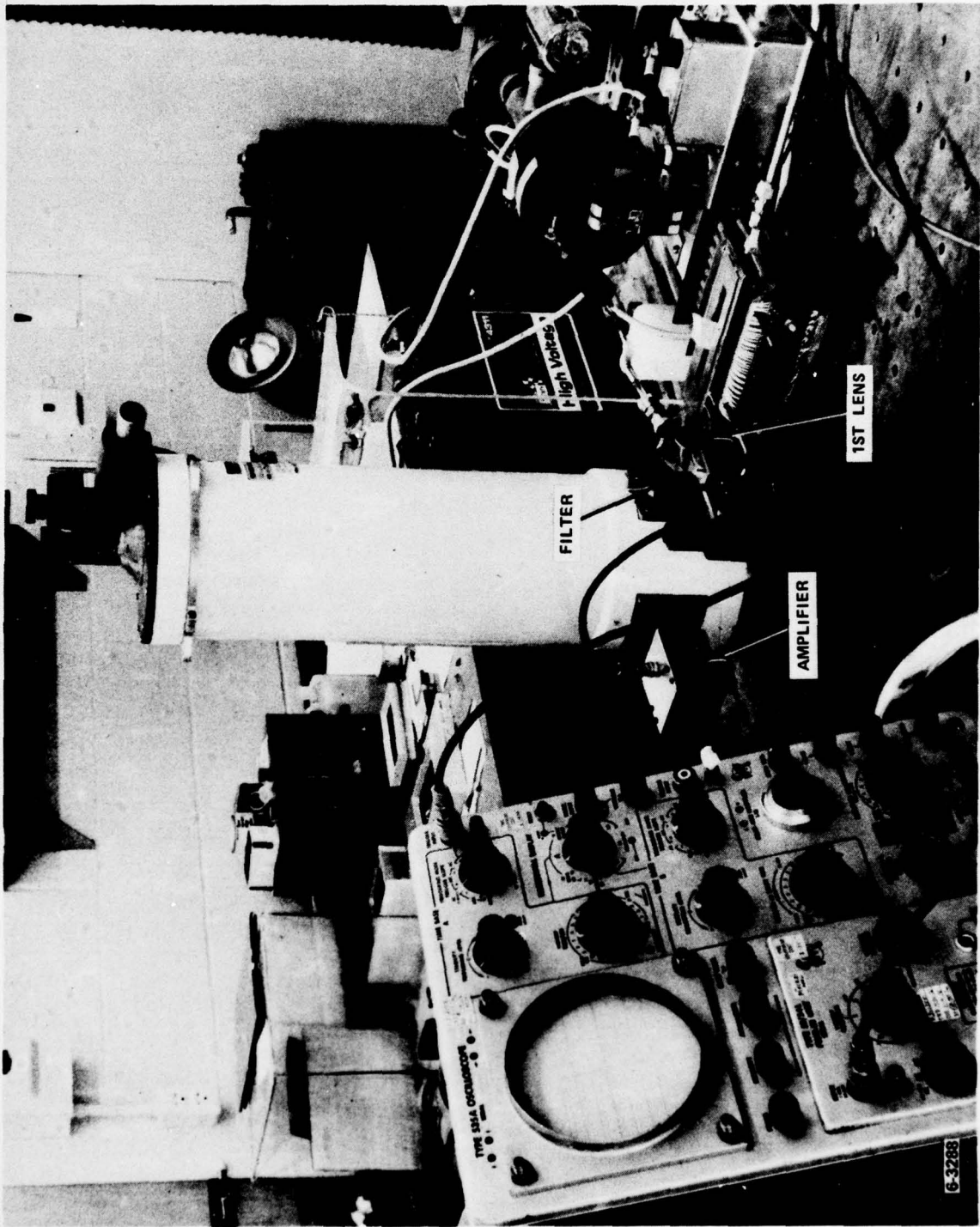
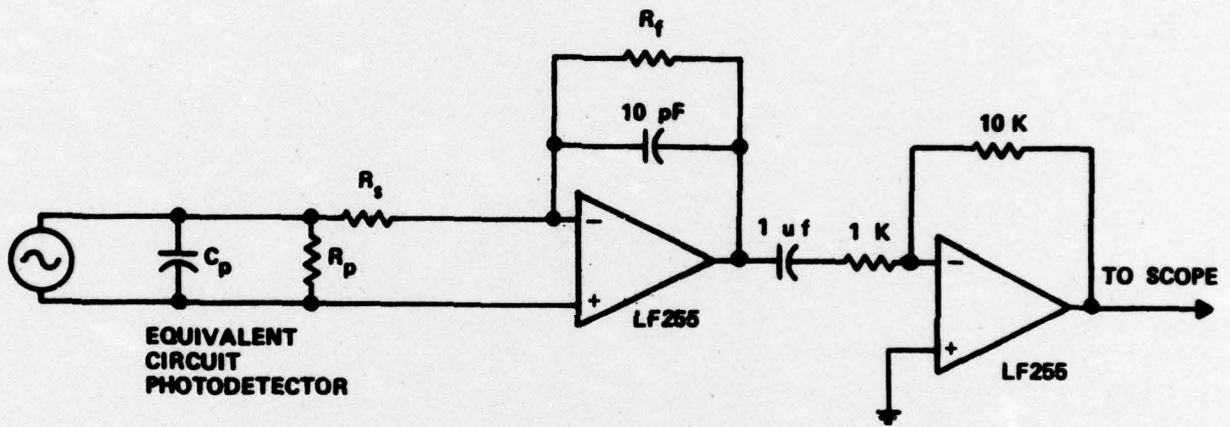


Figure 6. Fluorescence Radiometer

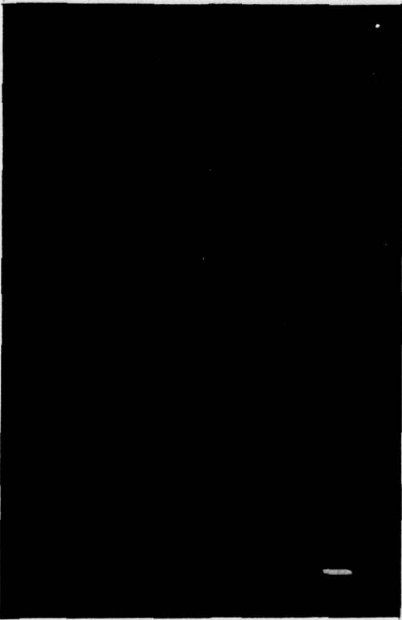


EQUIVALENT  
CIRCUIT  
PHOTODETECTOR

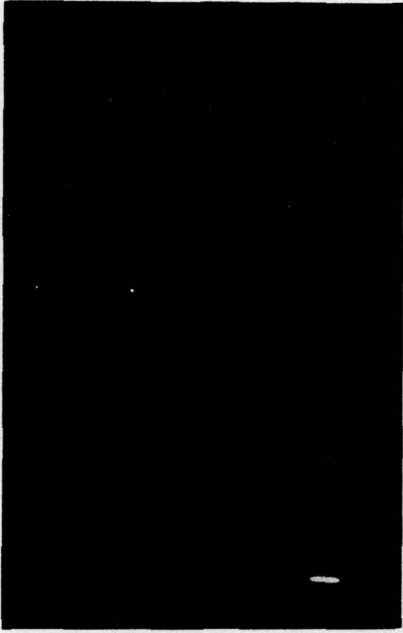
$R_p = 10 \text{ M}\Omega$   
 $R_s = 100 \Omega$   
 $C_p = 9 \text{ pF}$   
 $R_f = 68 \text{ K}\Omega$

6-3280

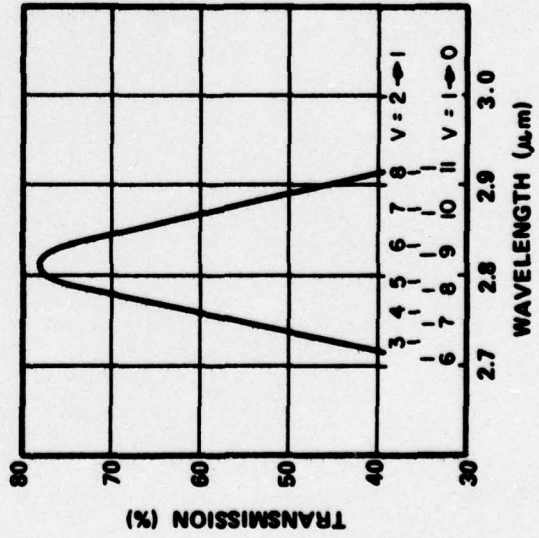
Figure 7. Photo Signal Amplifier



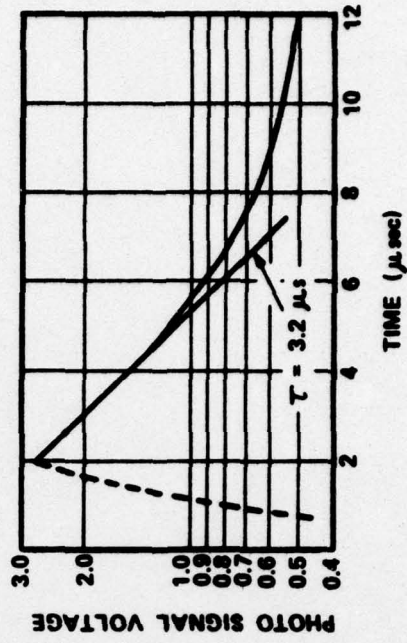
A. PHOTO SIGNAL - 275 Torr He ONLY



B. PHOTO SIGNAL - 275 Torr He + 5 Torr HF



C. SPECTRAL TRANSMISSION OF INTERFERENCE FILTER



D. SEMI-LOG PLOT OF PHOTO SIGNAL (B)

Figure 8. Fluorescence Data